Amino Acids (2015) 47:1091–1106
DOI 10.1007/s00726-015-1933-1

ORIGINAL ARTICLE

Proteome changes during yeast-like and pseudohyphal growth in the biofilm-forming yeast *Pichia fermentans*

Biancaelena Maserti · Alessandra Podda · Lucia Giorgetti · Renata Del Carratore · Didier Chevret · Quirico Migheli

Received: 31 August 2014 / Accepted: 3 February 2015 / Published online: 6 March 2015

Abstract The *Pichia fermentans* strain DISAABA 726 is a biofilm-forming yeast that has been proposed as biocontrol agent to control brown rot on apple. However, when inoculated on peach, strain 726 shows yeast-like to pseudohyphal transition coupled to a pathogenic behaviour. To identify the proteins potentially involved in such transition process, a comparative proteome analysis of *P. fermentans* 726 developed on peach (filamentous growth) vs apple (yeast-like growth) was carried out using two-dimensional gel electrophoresis coupled with mass spectrometry analysis. The proteome comparison was also performed between the two different cell morphologies induced in a liquid medium amended with urea (yeast-like cells) or methionine (filamentous cells) to exclude fruit tissue impact on the transition. Seventy-three protein spots showed significant variations in abundance (±twofold, $p < 0.01$, confidence intervals 99 %) between pseudohyphal vs yeast-like morphology produced on fruits. Among them, 30 proteins changed their levels when the two morphologies were developed in liquid medium. The identified proteins belong to several pathways and functions, such as glycolysis, amino acid synthesis, chaperones, and signalling transduction. The possible role of a group of proteins belonging to the carbohydrate pathway in the metabolic re-organisation during *P. fermentans* dimorphic transition is discussed.

Keywords Antagonistic yeast · Biological control · Dimorphic transition · Yeast proteome · *Candida lambica* · Two-dimensional electrophoresis

Introduction

In the past 20 years, knowledge of the negative impact of pesticides on the environment and human health and the

Handling Editor: P. R. Jungblut.

Electronic supplementary material The online version of this article (doi:10.1007/s00726-015-1933-1) contains supplementary material, which is available to authorized users.

B. Maserti (✉) · A. Podda
CNR-IPSP, Consiglio Nazionale delle Ricerche-Dipartimento di Scienze Bio-Agroalimentari, Istituto per la Protezione Sostenibile delle Piante, Area della Ricerca CNR, Via Madonna del Piano 10, 50019 Sesto Fiorentino, Florence, Italy
e-mail: elena.maserti@ipsp.cnr.it

L. Giorgetti
CNR-IBBA, Consiglio Nazionale delle Ricerche-Dipartimento di Scienze Bio-Agroalimentari, Istituto di Biologia e Biotecnologia Agraria, Area della Ricerca CNR, Via Moruzzi 1, 56124 Pisa, Italy

R. Del Carratore
CNR-IFC, Consiglio Nazionale delle Ricerche-Dipartimento di Scienze Biomediche, Istituto di Fisiologia Clinica, Area della Ricerca CNR, Via Moruzzi 1, 56124 Pisa, Italy

D. Chevret
INRA, UMR1319 Micalis, 78350 Jouy-en-Josas, France

D. Chevret
AgroParisTech, UMR Micalis, 78350 Jouy-en-Josas, France

Q. Migheli
Dipartimento di Agraria, University of Sassari, 07100 Sassari, Italy

Q. Migheli
Unità di Ricerca, Istituto Nazionale di Biostrutture e Biosistemi, University of Sassari, Viale Italia 39, 07100 Sassari, Italy

public pressure to reduce the use of chemical input on agricultural systems has emphasised the need to find alternative means to control post-harvest diseases of fruits and vegetables (Wisniewski and Wilson 1992; Lima et al. 1999). To this purpose, biological control by microbial antagonists has emerged as one of the most promising alternatives. The use of biofilm-forming yeast as effective antagonists has been given to a remarkable attention (Droby et al. 2009). However, biofilm formation in yeast should be regarded with care, as it is controversial whether the yeast or hyphal form is the most aggressive towards the host tissues. The so-called "strange case" of *P. fermentans* strain DISAABA 726 (Giobbe et al. 2007) emphasised the need for a deep assessment of candidate microbial antagonists to assure the safe use of any novel biocontrol agent. This strain proved an excellent antagonist towards brown rot caused by the pathogenic fungus *Monilinia* spp. on apple, but when inoculated on peach fruits, it unexpectedly displayed a pathogenic behaviour, causing rapid decay of fruit tissues even in the absence of *Monilinia* spp. By scanning electron microscopy techniques, *P. fermentans* 726 was shown to retain its yeast-like morphology when sprayed onto apple fruit, but upon inoculation on peach fruit, it underwent transition from budding growth to filamentous growth, suggesting that this morphology may be involved in the pathogenicity of *P. fermentans* 726 on peach tissue (Giobbe et al. 2007).

Critical depletion of nutrients often induces dimorphic switch to filamentous growth, characterised by branching networks of cell chains or hyphae to form a mycelium (Gancedo 2001). Filamentous growth should be considered an important adaptive response that functions analogously to cell motility by allowing a starving fungal colony to seek for nutrients (Lee and Elion 1999). Branching elements permit wider exploration of the environment at a lower energy cost than non-filamentous growth. Hence, the ambiguous behaviour of *P. fermentans* 726 could be related to induction of different genes by environmental factors, such as nutrient conditions peculiar to each fruit species. Characterisation of the differentially expressed genes during yeast-like to pseudohyphal transition may help to understand the biology of this peculiar yeast model. To this purpose, Fiori et al. (2012) identified several genes which differentially expressed between yeast and filamentous growth developed on fruit tissues. Additionally a proteomic approach could be also useful for elucidating the transition processes in *P. fermentans.* Proteomics has been successfully applied to study the effect of temperature on the proteome of *P. pastoris* (Dragosits et al. 2009) and the yeast-to-hypha transition in *Candida albicans* (Monteoliva et al. 2011). To the best of our knowledge, a study on the proteome changes in the two morphologies of *P. fermentans* has not yet been carried out. Hence, the aim of this work was to compare the proteome profile of yeast-like and filamentous morphologies of *P. fermentans* 726 to identify the proteins potentially involved in the yeast-filamentous cell switch.

Experimental

Organism and maintenance of yeast strain

P. fermentans Lodder [anamorph: *Candida lambica* (Lindner & Genoud) Uden & H.R. Buckley ex S.A. Mey. & Ahearn (1983)] DISAABA 726 (=DBVPG 3627) was isolated from wine must and maintained in the culture collection of the 'Dipartimento di Agraria', University of Sassari, Italy, in YEPD (2 % glucose, 2 % peptone, 1 % yeast extract, 2 % agar) at 4 °C for short-term storage, and in YEPD plus 20 % glycerol at −80 °C for long-term storage.

P. fermentans DISAABA 726 was precultured overnight at 25 °C in YEPD. The cells were then rinsed twice in sterile distilled water, inoculated on solid (5 × 106 cells) or liquid (5 × 106 cells mL^{-1}) media, and incubated statically at 25 °C.

Induction of dimorphic switch on liquid medium

Single yeast cells and filamentous growth were sampled using a Singer MSM micromanipulator (Singer Instruments Co. Ltd., Somerset, UK), plated onto either YCBU (YCB plus 0.2 % urea) or YCBM (YCB plus 0.2 % methionine) and incubated at 25 °C while being observed for up to 3 days according to Sanna et al. (2012).

Induction of yeast-like and pseudohyphal growth on apple and peach fruits

Samples of yeast-like and pseudohyphal-like cells of *P. fermentans* were grown on apple and peach fruits, respectively, as described by Fiori et al. (2012). Briefly, a single, fresh colony of *P. fermentans* DISAABA 726 was inoculated into a flask containing 30 mL of 1 % yeast extract, 2 % bacto peptone, 2 % dextrose broth (YPD) and incubated for 24 h at 25 °C on a rotary shaker (200×*g*). Cells were then recovered by centrifuging at 3,000×*g* for 5 min, washed and suspended in sterile Ringer's solution (H2O, 0.9 % NaCl) and brought to a final concentration of 1 × 109 cells mL^{-1} by direct counting with a hemocytometer. One hundred microliters of this suspension was spread between two autoclaved circular sheets of cellophane membrane backing sheets (Bio-Rad, Hercules, CA) permeable to liquids and nutrients, which were then placed between either on apple or peach fruits (Supplementary Fig. S1). Fruits selected for the study were at the same maturity and had been disinfected in sodium hypochlorite (0.8 %

as chlorine) and air-dried prior to being halved. A total of 66 each of apple and peach fruits were treated to recover a high quantity of yeast cells. The fruits were stored for 24 h at 25 °C at 85 ± 5 % relative humidity and then the yeast was scraped from the cellophane sheets with a sterile spatula, collected in 1.5-mL Eppendorf tubes and immediately frozen in liquid nitrogen and stored at −80 °C until further processing.

Preparation of *P. fermentans* DISAABA 726 total protein extracts

A total of 50 mg of yeast or filamentous cells were washed in PBS buffer and collected by centrifugation. Then the cells were broken in a mortar and pestle with acid-washed glass beads and liquid nitrogen. The powder was suspended in 150 µL extraction buffer and incubated for 20 min at 25 °C with vortexing at 5-min intervals. The extraction buffer contained 50 mM Tris, pH 8.8, 10 % glycerol, 7 M urea, 2 M thiourea, 1 % Triton X-100, 1 % SB 3-10, 20 mM EDTA, 2 % IPG buffer 3-10, 1 mM PMSF, and 50 mL *per* gram cells of protease inhibitor cocktail. The mixture was centrifuged for 20 min at 15,000 rpm and 18 °C. Following extraction, interfering components were removed using 2D-Clean Kit™ (GE-Healthcare). The pellet was suspended in 2 mM Tris, 7 M urea, 2 M thiourea, 4 % v/w CHAPS, 1 % IPG buffer 4–7 and subjected to a first step of reduction/alkylation before IEF, according to Herbert et al. (2001). Briefly samples were reduced by 5 mM TBP (Tributylphosphine Stock Solution, Sigma-Aldrich, Italy) for 1 h, followed by alkylation with 30 mM IAA for 3 h, in the dark. The protein concentration was determined using the RC-DC Protein Assay Kit (BioRad).

Two-dimensional gel electrophoresis (2-DE)

2-DE analysis was carried out using the gradient pH 4–7 linear IPG strips (GE Healthcare) for the isoelectric focusing. IPG strips (18 cm) were rehydrated for 6 h in passive mode and 6 h in active mode (50 V) at 22 °C in 350 µL of rehydration/sample buffer containing *P. fermentans* yeast-like or filamentous growth extracts (approximately 450 µg expressed as total proteins were loaded). IEF was carried out using the PROTEAN® IEF Cell System (BioRad) under the following conditions: Step 1, 250 V for 60 min; Step 2, 500 V for 120 min; Step 3, 500–1,000 V for 4 h; Step 4, ramped to 8,000 V for 4 h; and Step 3, 8,000 V for a total of 55,000 V/h. Strips were then equilibrated first for 15 min in a reducing solution (6 M urea, 50 mM Tris-HCl pH 8.8, 30 % v/v glycerol, 2 % w/v SDS and 2 % w/v DTT) and then 15 min in an alkylating solution (6 M urea, 50 mM Tris-HCl pH 8.8, 30 % v/v glycerol, 2 % w/v SDS and 4 % w/v iodoacetamide). Equilibrated IPG strips were then placed and fixed using agarose on the top of home-made 12 % SDS-polyacrylamide gels. Protein separation in the second dimension was carried out in a Protean XL cell (BioRad). The protein spots were visualized by staining with BioSafe Coomassie gel stain (BioRad), following manufacturer's instructions.

Image acquisition and statistical analysis

After de-staining, the gels were scanned using a GS-800 densitometer (BioRad) at 600 dpi resolution. To ensure a good statistical power, each experiment group (*P. fermentans* developed on YCBU, YCBM, apple, or peach fruits) contained five biological replicates for each morphology and each inducing condition, generating a total of 20 individual gels. Computerised analysis was performed matching the gel images by means of Redfin Solo software (www.ludesi.com). Comparisons were carried out between filamentous *versus* yeast morphology whatever the inducing strategy. Spot volume was calculated as integration of spot area. In order to reduce errors due to slight differences in gel staining or protein concentration, the volume of each spot was divided for the sum of the volume of all spots detected on gels to obtain normalised spot volume (% V). To find the differentially abundant proteins, statistical analysis was carried out using the web-based NIA array software tools (lgsun.grc.nia.nih.gov) (Sharov et al. 2005). The software selects statistically valid protein spots based on analysis of variance (one-way ANOVA). The raw data set was loaded on NIA and after indication of biological replications and transformation in log10, the data were analysed using the following settings: error model "max (average, actual)", 0.01 proportion of highest variance values to be removed before variance averaging, 10 degrees of freedom for the Bayesian error model, 0.05 FDR threshold, and zero permutations. Pairwise comparison of protein spot mean abundance values were performed with the software tools using the following settings defining differentially abundant proteins: confidence intervals 99 %, P value <0.01, twofold change threshold. To explore the association between protein abundance and morphology, hierarchical clustering was undertaken using the average distance method. Also, principal component analyses (PCA) were carried out using the following settings: correlation matrix type, three principal components, twofold change and 0.7 correlation threshold for clusters.

Biological processes and functions involving differentially abundant proteins

The biological processes and molecular functions associated with the differentially abundant proteins were inferred by searching on UniprotKb database (www.uniprot.org).

Protein identification by LC-MS/MS

Spots of interest were excised from preparative gels. In-gel digestion was performed with the Progest system (Genomic Solution) according to a standard trypsinolysis protocol. Gel plugs were first washed twice with 10 % (v/v) acetic acid, 40 % (v/v) ethanol in water, and then with acetonitrile. They were further washed with 25 mM NH4CO3 and dehydrated in acetonitrile (two alternating cycles). Following reduction (10 mM DTT, 1 h at 57 °C) and alkylation (55 mM idodacétamide, 45 min at 20 °C), digestion was performed for 6 h at 37 °C with 125 ng of modified trypsin (Promega) dissolved in 20 % (v/v) methanol in 20 mM NH4CO3. Tryptic peptides were first extracted with 50 % (v/v) acetonitrile, 0.5 % trifluoroacetic acid in water, and then with pure acetonitrile. Both peptide extracts were pooled, dried in a vacuum speed concentrator, and suspended in 25 µL of 2 % (v/v) acetonitrile, 0.08 % (v/v) trifluoroacetic acid in water.

Liquid chromatography was performed with a NanoLC-Ultra Eksigent system. The sample (4 µL) was loaded at a flow rate of 7.5 µL/min into a precolumn cartridge (20 mm, 100 µm internal diameter; stationary phase, Biosphere C_{18}, 5 µm; NanoSeparations, Nieuwkoop, The Netherlands) and desalted with 0.1 % (v/v) formic acid and 2 % ACN. After 3 min, the precolumn cartridge was connected to the separating column (150 mm, 75 µm internal diameter; stationary phase, Biosphere C_{18}, 3 µm; NanoSeparations). The buffers used were H_2O (buffer A) and ACN (buffer B) each containing 0.1 % (v/v) HCOOH. Peptides were separated using a linear gradient from 5 to 95 % B for 37 min at 300 nL/min. A single run took 45 min, including the regeneration step in 100 % buffer B and the equilibration step in 100 % buffer A. Eluted peptides were analysed online with an LTQ XL ion trap (Thermo Electron) using a nanoelectrospray interface. Ionisation (1.5 kV ionisation potential) was achieved with a liquid junction and an uncoated capillary probe (10 µm internal diameter; New Objective, Cambridge, MA, USA). Peptide ions were analysed using Xcalibur 2.0.7, with the following data-dependent acquisition steps: (1) full MS scan (mass-to-charge ratio *m/z* 400–1,400, centroid mode) and (2) MS/MS (qz = 0.25, activation time = 30 ms, and collision energy = 35 %; centroid mode). Step 2 was repeated for the three major ions detected in step 1. Dynamic exclusion was set to 45 s. The raw mass data were first converted to mzxml with the ReAdW sofware (SPC Proeomic Tools, Seattle, USA). Protein identifications in a *Pichia* genius database (Uniprot, 2010/09/15) were performed using the X! Tandem pipeline sofware (http://pappso.inra.fr/bioinfo/xtandem-pipeline) with the following parameters: enzymatic cleavage was declared as a trypsin digestion with one possible miscleavage event. Cys carboxyamidomethylation and Met oxidation were set to static and possible modifications, respectively. Precursor mass and fragment mass tolerance were 1.0 and 0.5 Da, respectively. A refinement search was added with similar parameters, except that semitryptic peptide and possible N-terminal amino acid acetylation, dehydratation, or deamidation was searched.

Identified proteins were filtered and grouped according to the following specifications: (1) at least two different peptides with an *E* value of <0.01 and a protein *E* value (calculated as the product of unique peptide *E* values) of $<10^{-4}$. In the case of identification with only two or three MS/MS spectra, the similarity between the experimental and theoretical MS/MS spectra was checked visually. In the absence of positive identification by mass matching, due to the fact that *Pichia fermentans* genome has not been sequenced, peptide sequences were determined by de novo interpretation of MS/MS spectra using DeNovo pipeline software (http://pappso.inra.fr/downloads/archives/DeNovo_pipeline_v1.4.4/). Only sequences containing a tag of at least six amino acids with an associated probability greater than 0.9 were selected. Sequence similarity was searched in the *Pichia* genius database and in a *Fungi* kingdom database (Uniprot 2011.05.30). Sequences corresponding to keratins or trypsin were first removed by querying a homemade contaminant database. Protein identifications were validated with a minimum of two independent peptides and an *E* value of <0.001. In all cases, the automatic de novo interpretation of MS/MS spectra was confirmed visually. The mass spectrometry proteomics data have been deposited to the ProteomeXchange Consortium (Vizcaíno et al. 2014) via the PRIDE partner repository (Vizcaino et al. 2013) with the dataset identifier PXD001664".

RNA extraction and semi-quantitative PCR (sqPCR)

Five proteins identified by mass spectrometry analysis were validated by sqPCR (Supplementary Table S1). The cDNA sequences used were found in Gene Bank starting from the peptides matching the selected proteins. The web-based Primer3 software provided by the Whitehead Institute at Massachusetts Institute of Technology was used to design the primers (Supplementary Table S2).Total RNA extraction was performed modifying the method suggested for the Taqman® Gene Expression Cells-to-CT™ Kit (Applied Biosystems). 10 mg of liquid-nitrogen frozen yeast or filamentous cells was extracted with PBS; 5 µL of the extracted suspension were added to lysis buffer plus DNase to exclude genomic contamination as described by the manufacturer. 2 µL of the reverse transcribed samples was used for PCR amplification performed with GoTaq® Green Mastermix (Promega, USA). As the Applied Biosystems

extraction method was performed for cell culture we validated the method using a standard RNA extraction procedure (Quiagen). The following standard thermal profile was used for all PCRs: 93 °C for 3 min; 33 cycles of which 93 °C for 30 s, 54 °C for 40 s, and 72 °C for 50 s; 72 °C for 5 min as final extension.

PCR products were separated by 1 % agarose gel electrophoresis and stained with ethidium bromide. cDNA fragments were purified from gels and sequenced by BMR-Genomics (Italy). For each PCR, the concentration of cDNA and the number of cycles were optimised to observe a quantifiable signal within the linear range of amplification, according to the putative level of each mRNA amplified and the size of the corresponding PCR product. Control reactions were performed in the absence of reverse transcriptase. Transcript levels were compared with 18S rRNA gene.

Actin immunostaining analysis

Immunostaining analysis of actin was performed with Phalloidin-TRITC staining: yeast-like and pseudohyphal cells of *P. fermentans* DISAABA 726 were fixed in 4 % paraformaldehyde without full drying for 30 min, rinsed with PBS three times, and incubated in a solution of 0.1–0.2 μg/mL phalloidin labelled with TRITC (Tetramethyl Rhodamine Isothiocyanate, Fluka 77418) in PBS in

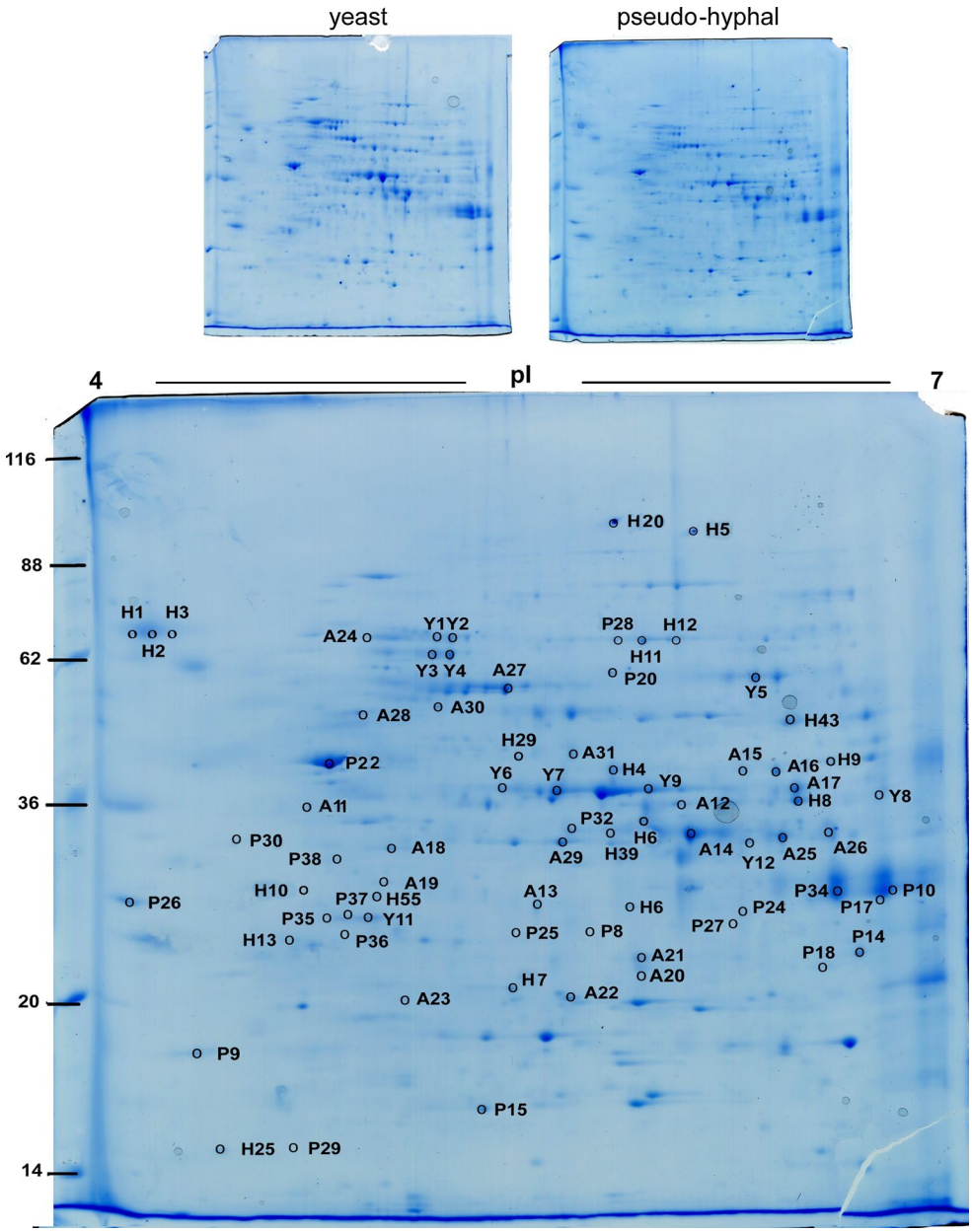

Fig. 1 Representative 2-DE patterns of protein extracted by *P. fermentans* strain DISABAA 726 in yeast and filamentous morphology. Proteins were separated on a 4–7 pH linear gradient in the first dimension (IEF) and 12 % SDS-polyacrylamide gels in the second dimension. Spot IDs correspond to those listed in Table 1a–d and supporting information Table S3. Label A_x indicates the proteins increased in abundance in yeast morphology developed on apple; Y_x indicates the proteins increased in abundance in yeast morphology developed both on apple and in YCBU; P_x indicates the proteins increased in abundance in filamentous morphology developed on peach; H_x indicates the proteins increased in abundance in filamentous morphology developed both on peach and in YCBM. Differentially abundant spots with at least twofold-change ratio and FRD <0.01 were used for calculation

the dark at room temperature for 1 h. After three rinses in PBS, the slides were coverslipped using antifading mounting fluid (Millipore). Cell wall staining was performed in yeast-like and pseudohyphal cells of *P. fermentans* DISAABA 726 with Lectin-Fluorescein isothiocyanate conjugate, from Canavalia ensiformis (Conc A) powder, 61761, Sigma-Aldrich (200 μg/mL in PBS, pH 7.4), according to the manufacturers' instructions, and incubated for 90 min in the dark at 30 °C.

Results

2-DE separation and identification of *P. fermentans* proteins

Total protein extracts of *P. fermentans* DISAABA 726 were analysed by 2-DE to detect the differentially abundant proteins between yeast and filamentous cells. First, the two morphologies were induced both on apple and peach fruits (Supplementary Fig. S1). Additionally, a simplified liquid medium was used to minimise the possible interference of the complex fruit environment (Sanna et al. 2012), yeast-like morphology being induced in liquid medium enriched of urea (YCBU), whereas the filamentous form was obtained after inoculating on methionine-enriched medium (YCBM) (Supplementary Fig. S1).

Computerised analysis showed around 930 protein spots in both yeast and filamentous morphologies, whatever the induction strategy (Supplementary Fig. S2). The proteome maps were reproducible and presented about 789 ± 67 matches between the two morphologies. After statistical analysis, a total of 110 protein spots were excised from the protein gels and analysed by LC-MS/MS analysis (Supplementary Table S3).

Differential protein spots in yeast and filamentous morphologies of P. *fermentans* DISAABA 726 were induced in apple and peach fruits

The comparison of the proteome of filamentous and yeast cells induced during growth on apple and peach fruits showed 73 protein spots whose abundance was changed significantly (Fig. 1).

Out of 73 identified protein spots, 41 showed an increase in abundance in the filamentous form, whereas the other 32 were more abundant in the yeast morphology (Table 1a–d).

Differential protein spots in the two *P. fermentans* DISAABA 726 morphologies induced by liquid medium

Among the 73 differentially abundant proteins observed during growth in fruit tissue, 30 proteins were also found to change in their abundance in *P. fermentans* DISAABA 726 when the dimorphic transition was induced by liquid medium. Eleven of these proteins were more abundant in the yeast form, while 19 in the filamentous form (Table 1a–d).

Multivariate analysis

In order to understand the relationship between the protein abundance and the different morphologies, hierarchical clustering and PCA were undertaken using data from 2-DE separation. The hierarchical clustering of the experiments highlighted that yeast cells clustered together, whatever the induction strategy and had protein abundance profiles different from those of pseudo-hyphal cells (Fig. 2a). On the other hand, hierarchical clustering among replicates showed a good correlation within replicates (Supplementary Fig. S3). PCA displays the principal components that distinguish among sources of variation within a dataset. In this work PC1, representing 53.9 % of variance, showed a clear separation between protein profiles from pseudohyphal morphologies which clustered in the left quadrants and those from yeast morphologies, clustering in the right quadrants. PC2, which represents 29.6 % of the variance, displays the separation between the two inducing strategies. PC3, representing 16.3 % of the variance, underlines the similarity between the protein profiles of different morphologies (Fig. 2b and Supplementary Fig. S4).

Functional analysis of the differentially abundant proteins

The 73 differentially abundant proteins in the different strategies were classified according the biological processes and the molecular function inferred by UniprotKB database. The most represented proteins in yeast cells belong to glycolysis/gluconeogenesis (38 %), aminoacid synthesis (19 %), and protein folding (13 %), whereas in the filamentous form there was not a prevalence of one process over the others (Fig. 3).

Several proteins, such as mitochondrial matrix ATPase, enolase, triosephosphate isomerase, mitochondrial ketoil-acid reductoisomerase, and alcohol dehydrogenase were found in more than one spot of the same yeast morphology.

Table 1 Proteins whose abundance changed in *P. fermentans* DISAABA 726 developed on apple fruits and YCBU (yeast form) or peach fruits and YCBM (filamentous form). The confidence intervals were 99 ‰. Underlined IDs indicate the proteins also tested with other techniques

Spot ID[a]	Accession[b]	Reference protein[c]	Reference organism[d]	Biological process[e]	Molecular function[f]	MW[g]	pI[g]	Protein profile[i]	P/A[j]	Protein profile[k]	M/U[l]
					YEAST FORM						
Protein folding											
Y1	C4R4C3	Mitochondrial matrix ATPase	*Pichia pastoris*	Protein folding	ATP binding	69.6	5.4		3.8		-5.6
Y2	C4R4C3	Mitochondrial matrix ATPase	*P. pastoris*	Protein folding	ATP binding	69.6	5.4		-4.7		-2.2
A24	C4R4C3	Mitochondrial matrix ATPase	*P. pastoris*	Protein folding	ATP binding	69.6	5.4		-2.4		
Response to stress											
Y3	A3LZ15	Heat shock protein HSP 70	*P. stipitis*	Response to stress	ATP binding	66.3	5.2		-2.0		-3.5
Y4	C4R5E4	Cytoplasmic ATPase, a ribosome associated molecular chaperone	*P. pastoris*	Response to stress	ATP binding	66.3	5.1		-3.4		-3.0
Glyoxylate pathway											
Y5	Q9HFN2	Isocitrate lyase	*P. jadinii*	Glyoxylate bypass Tricarboxylic acid cycle	Lyase	62.1	6.8		-5.9		-4.2
Glycolysis and gluconeogenesis											
Y6	A9YTT1	Enolase	*Issatchenzia orientalis*	Glycolysis Gluconeogenesis	Phosphopyruvate hydratase activity	40.5/45	4.9/5.5		-5.6		-2.1
A11	A9YTT1	Enolase	*I.orientalis*	Glycolysis Gluconeogenesis	Phosphopyruvate hydratase activity	40.6	4.9		-5.2		
Y8	A8J6W1	Phosphoglycerate kinase	*P. minuta*	Glycolysis Gluconeogenesis	Phosphoglycerate kinase activity	44.4	5.9		-8.4		-2.3
A20	C4R5P4	Phosphoglycerate mutase	*P. pastoris*	Glycolysis Gluconeogenesis	Phosphoglycerate mutase activity	28.2	6.0		-2.9		
A21	C4R5P4	Phosphoglycerate mutase	*P. pastoris*	Glycolysis Gluconeogenesis	Phosphoglycerate mutase activity	28.2	6.0		-2.9		
A22	C4R626	Triosephosphate isomerase	*P. pastoris*	Glycolysis Gluconeogenesis	Triose-phosphate isomerase activity	27.1	5.7		-2.5		
A23	A3LZL0	Triosephosphate isomerase	*P. stipitis*	Glycolysis Gluconeogenesis	Triose-phosphate isomerase activity	26.4	5.3		-2.5		
A25	Q92263	Glyceraldehyde-3-phosphate dehydrogenase	*P. pastoris*	Glycolysis Gluconeogenesis	NAD binding	35.5	6.5		-3.3		
A26	Q92263	Glyceraldehyde-3-phosphate dehydrogenase	*P. pastoris*	Glycolysis Gluconeogenesis	NAD binding	35.6	6.5		-2.2		
A31	A8J6W1	Phosphoglycerate kinase	*P. minuta*	Glycolysis Gluconeogenesis	Phosphoglycerate kinase activity	44.5	5.9		-3.5		
Y12	A3LQ70	Glyceraldehyde-3-phosphate dehydrogenase	*P. stipitis*	Glycolysis Gluconeogenesis	NAD binding	35.7	6.1		-4.5		-5.4
Y11	C4QW09	Fructose 1,6-bisphosphate aldolase	*P. stipitis*	Glycolysis Gluconeogenesis	Fructose-bisphosphate aldolase activity	23	4.2		-3.3		-3.2
Pentose shunt											
A29	A3M0D0	Transaldolase	*P. stipitis*	Pentose shunt	Transferase	35	5.2		-3.1		
Aminoacids synthesis											
A13	A3M0H4	Homo-isocitrate dehydrogenase	*P. stipitis*	Aminoacid biosynthesis Lysine biosynthesis.	Oxidoreductase	40.8	5.5		-4.1		
A15	A3LUW4	Mitochondrial ketoil-acid reductoisomerase	*P. stipitis*	Branched-chain amino acid biosynthetic process	Isomerase activity	44.3	6.9		-3.3		
		Mitochondrial ketoil-acid		Branched-chain amino							

Table 1 continued

Spot ID[a]	Accession[b]	Reference protein[c]	Reference organism[d]	Biological process[e]	Molecular function[f]	MW[g]	pI[g]	Protein profile[i]	P/A[j]	Protein profile[k]	M/U[l]
A16	A3LUW4	reductoisomerase	*P. stipitis*	acid biosynthetic process	Isomerase activity	44.3	6.9		-3.2		
A17	A3LS93	NADP-glutamate dehydrogenase	*P. stipitis*	Amino acid metabolic process	Oxido-reductase activity	44.3	6.9		-3.3		
Y9	A3M037	Glutamine synthetase	*P. stipitis*	Glutamine biosynthetic process	Ligase	49.2	5.9		33.4		2.1
Protein synthesis											
Y7	C4R4X4	Elongation factor Tu	*P. pastoris*	Protein biosynthesis	GTP binding	47.1	5.6		-4.2		-6.7
A19	A5DNL8	Elongation factor 1-alpha	*P. guilliermondi*	Protein biosynthesis	GTP binding	35.2	4.2		-3.3		
ATP synthesis											
A18	Q0ZIE5	ATP synthase subunit beta	*I. orientalis*	ATP synthesis Transport	ATP binding	36.1	4.8		-3.7		
A27	A5DECO	Vacuolar ATP synthase subunit B	*P. guilliermondi*	ATP synthesis Transport	TP binding	58.3	5.0		-5.9		
A28	A5DDN3	ATP synthase subunit beta	*P. guilliermondii*	ATP synthesis Transport	ATP binding	52.5	4.9		-2.2		
A30	C4R396	Vacuolar ATP synthase subunit B	*P. pastoris*	ATP synthesis process Transport	ATP binding	55.4	5.3		-4.3		
Cell cycle											
A12	Q9P8N0 B05	Mannose-1-phosphate guanyltransferase	*P. angusta*	Cell cycle	GTP binding	40.0	6.0		-4.1		
A14	Q9P8N0 B06	Mannose-1-phosphate guanyltransferase	*P. angusta*	Cell cycle	GTP binding	40.2	6.0		-3.3		
					PSEUDOHYPHAL FORM						
Protein folding											
H1	C4R4C3	Mitochondrial matrix ATPase	*P. pastoris*	Protein folding	ATP binding	69.6	4.2		26.8		14.8
H2	C4R4C3	Mitochondrial matrix ATPase	*P. pastoris*	Protein folding	ATP binding	69.6	4.2		13.2		10.9
Response to stress											
H12	A3LY16	Heat shock protein 70	*P.angusta*	Response to stress	Chaperone	70.3	5.1		7.6		5.4
H43	E7RB53	Ascorbate peroxidase	*P.angusta*	Response to oxidative stress	Oxidoreductase	39.3	5.6		15.2		13.1
H10	A3LXG8	Multifunctional chaperone (14-3-3 family)	*P.stipitis*	Response to stress	NA	29.2	4.6		10.3		9.8
Glycolysis											
H7	C4R5P4	Phosphoglycerate mutase	*P. pastoris*	Glycolysis Gluconeogenesis	phosphoglycerate mutase activity	27.6	5.3		7.9		4.1
P14	A3LQ70	Glyceraldehyde-3-phosphate dehydrogenase	*P. pastoris*	Glycolysis Gluconeogenesisis	NAD binding NADP binding	35.9	6.6		26.3		
P18	C4R0P1	Glyceraldehyde-3-phosphate dehydrogenase	*P. angusta*	Glycolysis Gluconeogenesis	NAD binding NADP binding	35.8	6.6		20.3		
Fermentation											
H9	O13309	Alcohol dehydrogenase	*P. stipitis*	Fermentation Ehrlich Pathway	Oxidoreductase	37.2	6.1		3.8		2.6
H11	O43106	Pyruvate decarboxylase Belongs to TPP family	*P. stipitis*	Fermentation Ehrlich Pathway	Pyruvate decarboxylase activity	61.2	5.5		5.6		6.7

Table 1 continued

Spot ID[a]	Accession[b]	Reference protein[c]	Reference organism[d]	Biological process[e]	Molecular function[f]	MW[g]	pI[g]	Protein profile[i]	P/A[j]	Protein profile[k]	M/U[l]
H39	O13309	Alcohol dehydrogenase	*P. stipitis*	Fermentation	Oxidoreductase	36.5	6.1	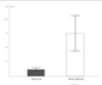	12.6		11.3
P28	C4R3T2	Major of three pyruvate decarboxylase Belongs to TPP family	*P.pastoris*	Fermentation Ehrlich Pathway	Pyruvate decarboxylase activity	61.4	5.6		5.1		
ATP synthesis											
P30	Q0ZIE4	ATP synthase subunit beta	*P. fermentans*	ATP synthesis	ATP binding	36	4.9	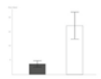	4.5		
Aminoacid synthesis											
H5	C4QZU2	Cobalamin—independent methionine synthase	*P. pastoris*	Methionine biosynthetic process	Methyltransferase activity	85.8	5.9	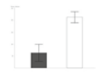	3.2		4.6
H20	A3LVA0	Methionine-synthesizing 5-methyltetrahydropteroyl triglutamate-homocysteine methyltrasferase	*P. stipitis*	Methionine biosynthetic process	Methyltransferase activity	85.5	5.3	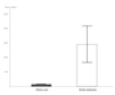	16.2		12.7
H6	C4R560	Thyazole synthase	*P. pastoris*	Thiamine biosynthetic process Adaptation to stress condition	Metal ion binding	37	6.0	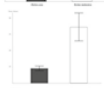	3.8		4.1
P20	C4R588	Asparagine synthetase	*P.pastoris*	Asparagin biosynthetic process	ATP binding	65	5.6	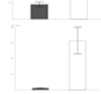	26.6		
P32	P34733	3-isopropylmalate dehydrogenase	*P.angusta*	Branched amino-acid biosynthesis Leucine biosynthesis	Dehydrogenase activity	37.9	5.2		6.2		
Phosphate metabolic processes											
P8	O13505	Inorganic pyrophosphatase	*P. pastoris*	Phosphate metabolic processes	Inorganic diphosphatase activity	32	5.5		24.7		
P25	A5DEU1	Inorganic pyrophosphatase	*P.guillermondii*	Phosphate metabolic processes	Inorganic diphosphatase activity	32	5.1		6.1		
Translation											
P9	A3GHD3	Nascent polypeptide-associated complex	*P. stipitis*	Translation	NA	19	4.8		25.5		
P10	C4R5H6	Protein component of the small (40S) ribosomal subunit	*P. pastoris*	Translation	RNA binding	25	9.3	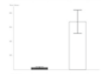	22.4		
P17	C4R5H6	Protein component of the small (40S) ribosomal subunit	*P. pastoris*	Translation	RNA binding	25	9.3		17.9		
P26	C4QYK0	40S ribosomal protein	*P.pastoris*	Translation	structural constituent of ribosome	29	4.6	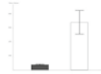	8.9		
Signal transduction											
H4	C4R4V8	cAMP-dependent protein kinase regulatory subunit	*P. pastoris*	Signal transduction	Kinase activity	44.7	5.5	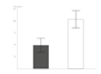	2.0		2.5
Cell cycle											
H25	Q96VU9	Cofilin	*P. angusta*	Cell cycle Cell division	NA	16.1	4.9	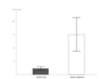	25.9	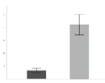	15.8
H8	A5DQP9	Actin	*P. guillermondii*	Cell cycle	ATP binding	42.2	6.3	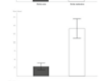	4.9		3.1
P29	Q96VU9	Cofilin	*P.angusta*	Cell cycle	NA	15.9	4.9		6.6		
Proteasome											
P22	A3LN33	26S proteasome regulatory particle	*P. stipitis*	Proteasome	NA	48.0	4.8	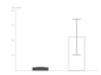	7.2		
P38	A3LPI7	Predicted protein	*P. stipitis*	Ubiquitin dependent protein catabolic process	Threonine-type endopeptidase activity	32.4	4.5	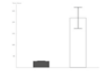	7.5		

Table 1 continued

Spot ID[a]	Accession[b]	Reference protein[c]	Reference organism[d]	Biological process[e]	Molecular function[f]	MW[g]	pI[g]	Protein profile[i]	P/A[j]	Protein profile[k]	M/U[l]
Unknown											
P24	A3LWH7	WD repeat protein	*P.stipitis*	Unknown	Unknown	34.5	5.6		4.5		
P27	A3LWH7	WD repeat protein	*P.stipitis*	Unknown	Unknown	34.5	5.6		6.1		
H55	C4R3X5	Primary component of eisosomes	*P.pastoris*	Unknown	Unknown	33.8	4.8		4.1		4.9
H13	A3GG33	Long chain base stimulates phosphorylation	*P. stipitis*	Unknown	Unknown	34	4.7		4.7		2.3
P35	C4R3X5	Primary component of eisosomes	*P.pastoris*	Unknown	Unknown	33.8	4.8		19.2		
P36	C4QXG9	Putative uncharacterized protein TRP repeat domain	*P.pastoris*	Unknown	Unknown	36.2	4.8		2.2		
P37	F2QN63	Small glutamine-rich tetratricopeptide	*P. angusta*	Unknown	Unknown	36	4.8		7.7		
No match											
H3		No match				70	4.2		33.3		30.5
P15		No match				16	5.0		3.6		
P34		No match				25	6.4		5.3		

[a] ID corresponds to spot position in the gel as illustrated in Fig.2. **A** indicates protein spots more abundant in the yeast form developed on apple fruits; **P** indicate protein spots more abundant in the filamentous growth developed on peach fruits; **Y** indicates protein spots more abundant in yeast form developed both on apple fruit and on YCBU; **H** indicated protein spots more abundant in the filamentous growth developed both on peach fruit and on YCBM.

[b] Protein accession number

[c] Reference protein (as inferred by Uniprotkb , www.uniprot.org)

[d] Reference organism (as inferred by Uniprotkb)

[e] Biological process in which the protein is involved as annotated in Uniprotkb

[f] Molecular function as annotated in Uniprotkb

[g] M W and p*I* indicate molecular mass and isoelectric point of the identified proteins, respectively

[i] Protein profile in yeast-like ■ and □ filamentous form of *P. fermentans* grown on apple or peach fruits; Vertical bars indicate the mean value (n=5) ±SE.

[j] Fold change in dimorphic transition induced on fruits : filamentous form (P) normalized volume/yeast form (A) normalized volume; more abundant proteins (≥ 2); less abundant proteins (≤ -2); confidence intervals 99%; *P* value < 0.01

[k] Protein profile in yeast-like ■ and ▒ filamentous form of *P. fermentans* grown on YCBU or YCBM; Vertical bars indicate the mean value (n=5) ±SE.

[l] Fold change in dimorphic transition induced in liquid medium: filamentous form(M) normalized volume/yeast form (U) normalized volume; more abundant proteins (≥ 2); less abundant proteins (≤ -2); Confidence interval 99%; *P* value < 0.01

Proteins also tested with other techniques: **By Fiori et al. (2012):** Heat shock protein HSP 70, phosphoglycerate kinase, elongation factor 1, and NADP(+)-dependent glutamate dehydrogenase were tested using RaSh; glyceraldehyde-3-phosphate dehydrogenase, enolase, thiazole synthetase and pyruvate decarboxylase were tested using PCR-select TM cDNA substraction. **In this work:** actin was tested by immunostaining (Figure 4A); the major of the three pyruvate decarboxylase, alcohol dehydrogenase, methionine-synthesizing 5-methyltetrahydropteroyl triglutamate-homocysteine methyltrasferase, multifunctional chaperone (14-3-3 family) and the primary component of eisosomes were tested by sqPCR (Figure 4B).

Differentially abundant proteins involved in energy production pathways

Several enzymes belonging to the glycolysis/gluconeogenesis pathway were found to be more abundant in yeast cells compared to filamentous ones. Also the isocitrate lyase belonging to glyoxalate cycle and the NADP-glutamate dehydrogenase showed higher abundance in yeast over filamentous cells. On the other hand, the pyruvate decarboxylase and alcohol dehydrogenase involved in alcoholic fermentation increased their abundance in filamentous cells. In the filamentous morphology, an increase in abundance of proteins involved in the biosynthesis of methionine and asparagine was also observed.

Interestingly, different species of two proteins, phosphoglycerate mutase and glyceraldehyde-3-phosphate dehydrogenase increased their abundance either in yeast or in filamentous morphology.

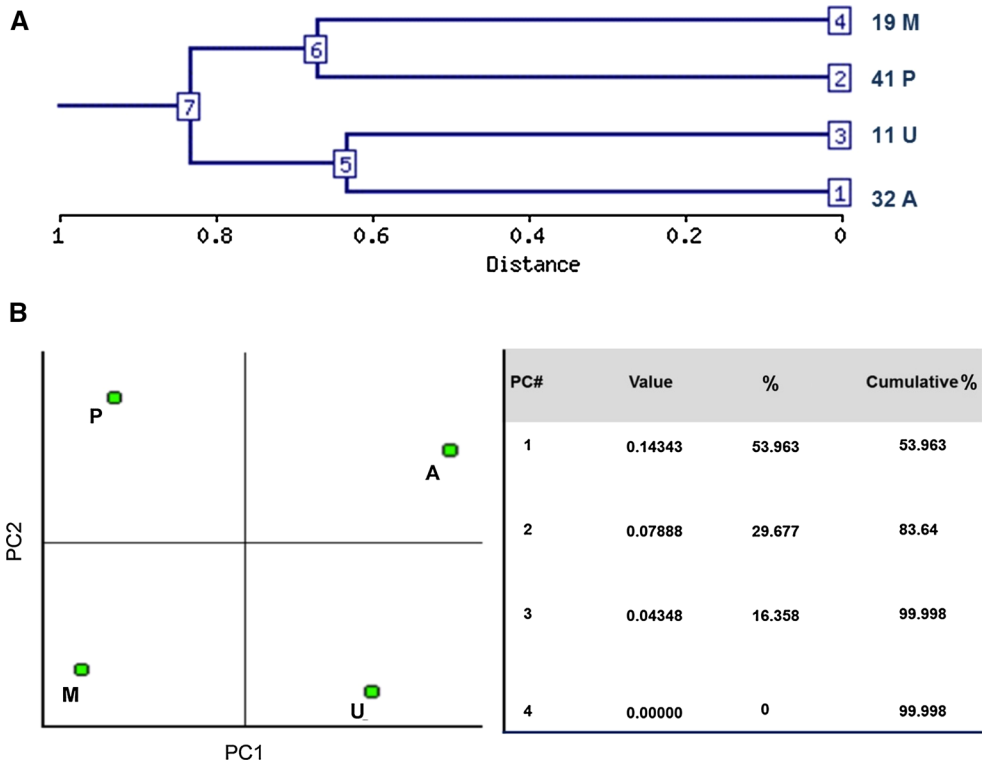

Fig. 2 **a** Dendogram showing the hierarchical clustering of the four experimental conditions: yeast cells induced in apple fruit (*A*); filamentous growth induced in peach fruit (*P*); yeast cells of *P. fermentans* DISAABA 726 induced in YCBU (*U*); filamentous growth induced in YCBM (*M*); **b** PCA and eigenvalues table diagram, as inferred by NIA Array Analysis Tool (www.lgsun.grc.nia.nih.gov): yeast cells of *P. fermentans* DISAABA 726 induced in apple fruit (*A*) or in YCBU (*U*), and filamentous growth induced in peach fruit (*P*) or in YCBM (*M*). Differentially abundant spots with at least twofold-change ratio and FRD <0.01 were used for calculation

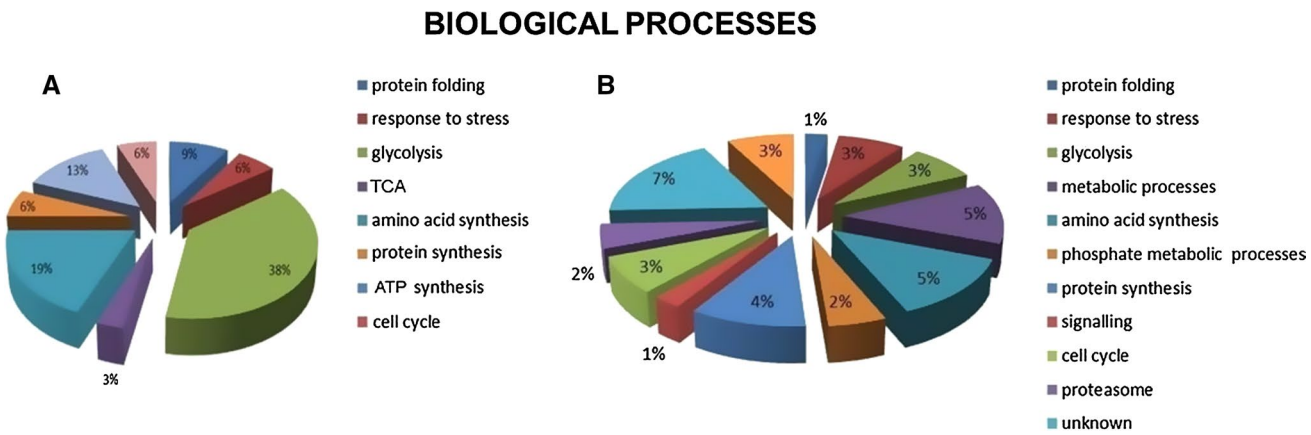

Fig. 3 Biological processes found increased in abundance in yeast (**a**) and filamentous growth (**b**) of *P. fermentans* DISAABA 726 as inferred by www.uniprot.org

Differentially abundant proteins related to other cellular processes

Actin was more abundant in filamentous cells developed on peach and on methionine (spot H8). Also other proteins, such as Hsp90 and Hsp70, which could be interconnected with actin were more abundant in filamentous cells. These proteins are generally known to be involved in protein folding, refolding, and stabilisation. Another actin-binding protein, the multifunctional chaperone belonging to the 14-3-3 family, has been found increased in filamentous cell.

Ascorbate peroxidase, a protein involved in the protection against oxidative stress and a principal component of eisosomes, was more abundant in filamentous than in yeast cells.

Validation of proteomic data by other techniques

The presence of actin was also tested by immunostaining analysis that confirmed the higher levels of the protein in the filamentous growth with respect to yeast cells (Fig. 4a). To validate the abundance levels of five proteins, the major

of the three pyruvate decarboxylase, alcohol dehydrogenase, methionine-synthesising 5-methyltetrahydropteroyl triglutamate-homocysteine methyltrasferase, multifunctional chaperone (14-3-3 family), and primary component of eisosomes, sqPCR analysis was performed using the respective peptide sequences identified by MS, as template for designing the primers. The transcript expression was positively correlated with the abundance profile of the respective protein and was higher in the filamentous growth than in yeast cells (Fig. 4b).

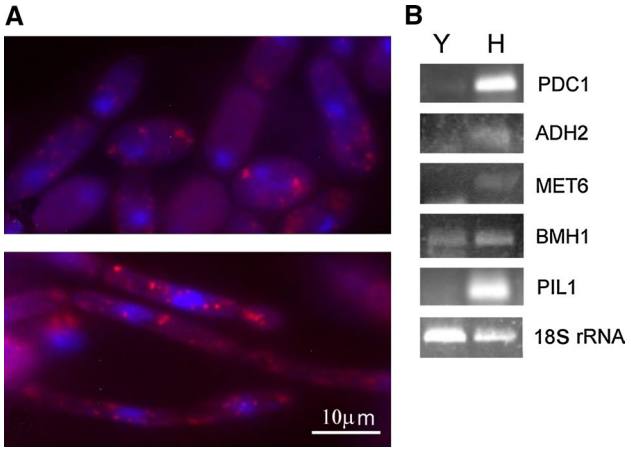

Fig. 4 Validation of proteomic data. **a** Image of actin in yeast cells induced in YCBU (*top*) and in filamentous growth induced in YCBM (*bottom*) obtained by immunofluorescence analysis; **b** sqPCR confirmation of abundance levels in yeast (*Y*) (*left*), and filamentous growth (*H*) (*right*) for the genes encoding the five selected proteins whose abundance was higher in filamentous growth than in yeast cells. Specific gene sequences were obtained using as template the peptide sequences of the proteins identified by MS analysis. The PCR products were obtained after 35 cycles of amplification. 18S rRNA was used as reference gene

Discussion

Yeasts may change their phenotype in response to environmental variations. The *P. fermentans* strain DISAABA 726 has been reported for its biocontrol properties against the brown rot pathogen *M. fructicola* on apple fruit. However, *P. fermentans* DISAABA 726 undergoes reversible morphological changes between yeast (spherical) and pseudo-hyphal (filamentous) forms of growth and displays pathogenic traits upon inoculation on peach fruits (Giobbe et al. 2007). This finding opens serious problems in the use of antagonistic yeasts. In this work the two yeast morphologies were compared by using 2-DE followed by MS, to identify the proteins which might be involved in the described dimorphic/pathogenic transition. The dimorphic switch was induced both by growing the yeast on apple or peach fruits (Fiori et al. 2012) and on liquid medium amended with urea or methionine, respectively (Sanna et al. 2012) to avoid interference due to the complex fruit environment.

The proteome profiles of yeast and filamentous morphologies were visually similar whatever the induction strategy (Supplementary Fig S2); however, statistical analysis showed differences in the abundance of 73 proteins between the two morphologies induced on fruits. Thirty of them also changed their abundance in the two morphologies developed on liquid medium.

The good similarity between the protein profiles of replicates from the same morphology, showed by the hierarchical clustering of the four experimental conditions, pointed out the reproducibility of the two induction strategies. Hierarchical clustering pointed out the distance between the protein profiles of yeast and filamentous cells. This distance was also confirmed by PC1 (Fig. 3; Supplementary Fig. S4). On the other hand as indicated by PC2, the two inducing strategies had minor impact on the proteome variation as indicated by PC2. The complexity of the fruit environment with respect to the simplified liquid medium may account for the higher number of differentially abundant proteins (73) found on *P. fermentans* grown on fruits compared to those found in cells developed on the liquid medium (30). The unexpected similarity between yeast and filamentous morphologies developed on different induction conditions displayed by PC3 (Supplementary Fig. S4) might be correlated to the increased abundance of several proteins such as glyceraldehyde 3 phosphate dehydrogenase and phosphoglycerate mutase both in yeast and filamentous morphologies (Table 1a–d). This behaviour might indicate that different species of the same protein might be involved in the dimorphic transition with different physiological relevance in the two morphologies (Jungblut et al. 2008; Schlüter et al. 2009). In *Candida albicans*, Monteoliva et al. (2011) suggested that phosphoglycerate mutase can function as glycolytic enzyme providing energy for the yeast growth morphology, whereas in the filamentous growth, phosphoglycerate mutase might provide glucose donor for the synthesis of β-glucans and chitin. Further investigations should be performed to understand the function of different protein species in the transition of *P. fermentans*.

As the aim of this work was to elucidate the molecular mechanism determining P. *fermentans* DISAABA 726 dimorphic transition, only the putative role of proteins showing differential abundance between the two morphologies, whatever the induction strategy, are discussed here. A model of metabolic changes taking place during *P. fermentans* DISAABA 726 dimorphic transition is also provided.

Carbohydrate pathway

Proteomic analysis showed a different organisation of the carbohydrate pathway in the two morphologies. Several proteins, belonging to glycolysis/gluconeogenesis pathway, increased in abundance in yeast morphology of *P. fermentans* as a consequence of the exponential growth phase of the yeast form, and in accordance with data reported by Monteoliva et al. (2011). This behaviour suggests that the yeast status is characterised by active aerobic glycolysis. Also the increased amount of isocitrate lyase, an enzyme involved in the glyoxylate pathway, was found in the yeast form. The glyoxylate cycle allows simple carbon compounds to be used in the synthesis of macromolecules including glucose, and its activation in *Pichia* yeast-like cells may be indicative of the modulation of the carbon flux in response to nutrient availability in the growth medium.

The higher levels of NADP-GDH in the yeast form with respect to the filamentous growth are not in accordance with the transcriptomic results reported by Fiori et al. (2012). However, discordance between mRNA expression and protein abundance has been previously reported by Chen et al. (2002). NAD- and NADP-dependent glutamate dehydrogenases occupy a key position in inter-linking the carbon and nitrogen metabolism in fungi. In *Benjaminella poitrasii*, Aradhana et al. (2004) observed a morphology-associated increase of NADP-dependent glutamate dehydrogenases during yeast-mycelium transition of a dimorphic fungus, while Joshi et al. (2010) suggested that a low ratio between NADP-GDH/NAD-GDH may have a role in the yeast-transition switch from aerobic to fermentation metabolism shunting pyruvate to acetaldehyde.

In the filamentous form, increased abundance of two enzymes, namely pyruvate decarboxylase and alcohol dehydrogenase required for the conversion of pyruvate to ethanol in the alcoholic fermentation pathway was found. This profile was also confirmed in this work by sqPCR for both pyruvate decarboxylase and alcohol dehydrogenase (Fig. 4). Additionally, transcriptomic analysis performed by Fiori et al. (2012) on yeast samples grown of fruits showed overexpression of the gene encoding pyruvate decarboxylase in filamentous morphology induced on peach fruit. The catalytic activity of pyruvate decarboxylase depends on the presence of the cofactor thiamine diphosphate (König et al. 2009) a derivative of thiamine. Synthesis of this compound requires thiazole synthetase, an enzyme which proved to be more abundant in the filamentous morphology of *P. fermentans* growing on peach fruit than in the yeast-like form growing on apple. Thiamine derivatives were suggested to be involved in the regulation of gene expression in response to adverse environmental conditions through as yet unidentified signal transduction pathways (Tylicki and Siemieniuk 2011). This observation suggests that the filamentous form of *P. fermentans* DISAABA 726 feeds itself using the fermentation pathway, as represented in the model of Fig. 5.

Ehrlich pathway and yeast-filamentous growth transition

In *P. fermentans*, the filamentous switch seems to be triggered by methionine, as demonstrated by the induction of pseudohyphal growth on a liquid medium enriched with this amino-acid (Sanna et al. 2012). Interestingly, Bremer et al. (1996) reported that in peach fruits the methionine content is higher than in apple fruit. Also, it was observed that the presence of methionine was the signal for the onset of the transition to filamentous growth in *Candida* (Maidan et al. 2005). It is well known that in particular conditions of restricted nitrogen supply, some amino acids such as methionine can be assimilated through the Ehrlich pathway, leading to the production of higher alcohol (Hazelwood et al. 2008). Dickinson (2008) showed that some fusel alcohols, which remain after most of the ethanol has been removed from any yeast fermentation, can promote an aberrant, elongated morphology in *S. cerevisiae*. Lorenz et al. (2000) characterised the connection between these alcohol-induced morphological changes and pseudohyphal growth. Several alcohols, notably isoamyl alcohol and butanol, promote a filamentous growth on solid medium and an elongated or filamentous form in liquid medium. Interestingly, pyruvate decarboxylase and alcohol dehydrogenase, which increased in abundance in the filamentous growth of *P. fermentans,* may also act in the Ehrlich pathway, suggesting that this pathway might be involved in the dimorphic transition of *P. fermentans*. Thus it may be hypothesised that the dimorphic transition in peach fruit tissue can be favoured by the uptake of methionine by *P. fermentans*. Unexpectedly, two enzymes involved in the biosynthesis of methionine were found increased in abundance in the filamentous growth developed both on peach fruits and on YCBM. Also, the transcript of methionine-synthesising 5-methyltetrahydropteroyl triglutamate-homocysteine methyltrasferase was found overexpressed in the filamentous form growth on YCBM. This finding suggests the intriguing hypothesis that filamentous form sustains itself by synthesising the substrate necessary for its survival.

Stress response

The levels of several proteins involved in stress response, such as ascorbate peroxidase and heat shock protein 70 (HSP 70), increased in filamentous form growth on peach fruits and on YCBM. These results are in accordance with transcriptomic analyses carried out by Fiori et al. (2012) that showed enhanced expression of several stress response genes in the filamentous growth on peach fruits. Zaragoza and Gancedo (2000) reported that filamentous growth is

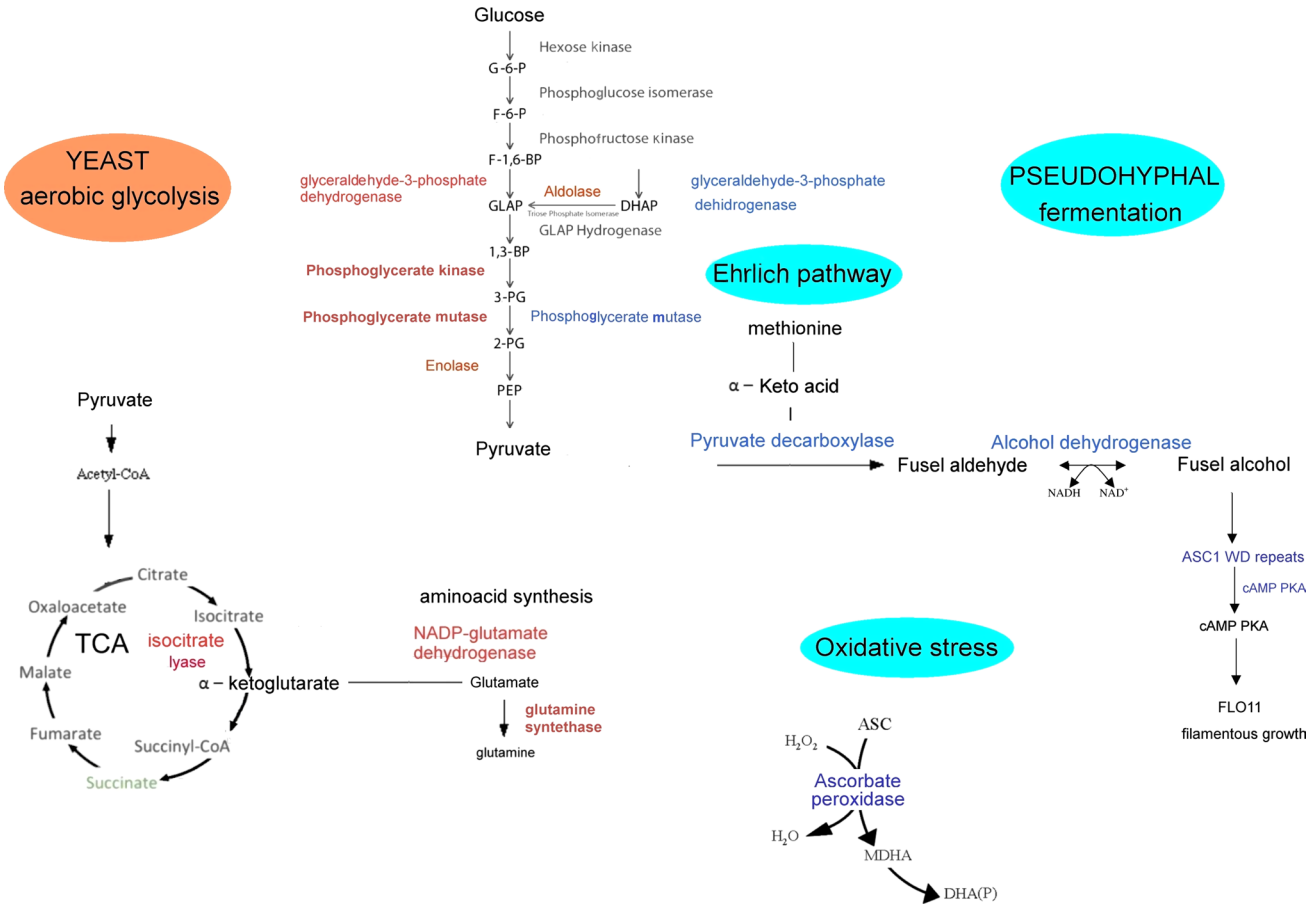

Fig. 5 Proposed model of metabolic changes taking place during *P. fermentans* dimorphic transition

a physiological response to both starvation and a stressful environment. In the first case, it would allow yeasts to forage for nutrients which may be present in the vicinity, and in the second case it would facilitate the escape from harmful agents. On the other hand, in the yeast form, the increased abundance of HSP 70 may act as molecular chaperone in assisting protein folding to prevent aggregation of unfolded polypeptides (Moraes Nicola et al. 2005).

Signal transduction

Two signalling pathways regulate filamentous growth of *S. cerevisiae* in nitrogen limitation (Zurita-Martinez and Cardenas 2005). One of the two pathways involves a nutrient sensing G-protein-coupled receptor that signals via cAMP and protein kinase A (Pan et al. 2000). In *P. fermentans*, a WD repeat protein (ACS1), which is similar to a G-protein receptor, may interact with the cAMP-dependent protein kinase, which is also increased in filamentous form, hence allowing this enzyme to integrate inputs from distinct signalling pathways. The ACS1 might be involved in the hyphal development and virulence of *P. fermentans*, as observed by Liu et al. (2010) in the human pathogen *C. albicans.*

Cytoskeleton formation and vesicular trafficking

During the hyphal development, fungi are characterised by polarised growth associated with the polarisation of the actin cytoskeleton. On the one hand, the higher content of actin and the associate protein cofilin in filamentous form of *P. fermentans* compared to yeast form may be requested to satisfy the need of more actin protein during the filament assembling (Han-Yaku et al. 1996). On the other hand, actin has been suggested to be involved in vesicular trafficking (Ayscough et al. 1997) and may interact with another protein that increased abundantly during filamentous, a 14-3-3-like protein. The 14-3-3 proteins are known to be involved in responses to diverse stresses in yeast (Van Hemert et al. 2001), as well as in various signal transduction pathways through controlling the activities of kinases and phosphatases. This function suggests that 14-3-3 proteins might regulate multiple pathways involved in the dimorphic transition of *P. fermentans* as has

been previously described for others yeast (Fu et al. 2000; Hurtado and Rachubinski 2002). The increase of actin and 14-3-3 protein in filamentous growth was also correlated with overexpression of the encoding genes.

Furthermore, in filamentous growth induced by peach, a major component of eisosomes was found increased in abundance as well as its mRNA transcript. The eisosomes are large protein complexes predominantly composed of BAR-domain-containing proteins Pil1 and its homologs are situated under the plasma membrane of ascomycetes. A successful targeting of Pil1 onto the future site of eisosomes accompanies their maturation. During or after recruitment, Pil1 undergoes self-assembly into filaments that can serve as scaffolds to induce membrane furrows or invaginations (Olivera-Couto and Aguila 2012). Although the physiological role of eisosomes in the dimorphic transition needs further investigation, these data might suggest that in *P. fermentans* the more complex filamentous organisation, with respect to the yeast one, requires an increase of cell-to-cell communication to redistribute cell biomolecules to a different location.

Conclusion

Pichia fermentans DISAABA 726 represents one of the very few cases ever reported of a yeast that displays a pathogenic behaviour on plant species (Giobbe et al. 2007). The results presented in this work indicate that the complex and finely tuned switch from yeast-to-filamentous growth of *P. fermentans* on peach might be driven by high levels of methionine and stress conditions present in peach fruits. A signal transduction pathway involving a putative nutrient sensing G-protein-coupled receptor, cAMP, and protein kinase might trigger the dimorphic switch.

Thus, besides the obvious implications in biological control and risk assessment studies, this yeast strain may represent a new model system to explore protein–protein interaction during dimorphic transition in microorganisms.

Pichia fermentans proteome

The mass spectrometry proteomic data have been deposited to the ProteomeXchange Consortium (Vizcaíno et al. 2014) via the PRIDE partner repository (Vizcaino et al. 2013) with the dataset identifier PXD001664.

Acknowledgments We are grateful to Dr. Stefano Fiori for carrying out the experiments on apple and peach fruits. This work has been granted by Ministry of Instruction and Research (MIUR) of Italy by PRIN07 project: evaluation of new risk factors associated with the utilisation of microbial antagonists.

Conflict of interest The authors declare that they have no competing financial interest.

References

Aradhana A, Mangesh J, Deshpand MV (2004) Morphology-associated expression of NADP-dependent glutamate dehydrogenases during yeast-mycelium transition of a dimorphic fungus *Benjaminiella poitrasii*. Antonie Van Leeuwenhoek 85:327–334

Ayscough KR, Stryker J, Pokala N, Sanders M, Crews P, Drubin DG (1997) High rates of actin filament turnover in budding yeast and roles for actin in establishment and maintenance of cell polarity revealed using the actin inhibitor latrunculin-A. J Cell Biol 137:399–416

Bremer HJ, Anninos A, Schultz B (1996) Amino acid composition of food products used in the treatment of patients with disorders of the amino acid and protein metabolism. Eur J Pedriatr 55:S108–S114

Chen G, Tarek G, Gharib TG, Huang C-C, Taylor JMG, David E, Misek DE, Kardia SRL, Giordano TG, Iannettoni MD, Orringer MB, Hanash SM, Beer DG (2002) Discordant protein and mRNA expression in lung adenocarcinomas. Mol Cell Proteomics 1:304–313

Dickinson JR (2008) Filament formation in *Saccharomices cerevisiae*. Folia Microbiol 53:3–14

Dragosits M, Stadlmann J, Albiol J, Baumann K, Maurer M, Gasser B, Sauer M, Altmann F, Ferrer P, Mattanovich D (2009) The effect of temperature on the proteome of recombinant *Pichia pastoris*. J Proteome Res 8:1380–1392

Droby S, Wisniewski M, Macarisin D, Wilson C (2009) Twenty years of postharvest biocontrol research: is it time for a new paradigm? Postharvest Biol Technol 52:137–145

Fiori S, Scherm B, Liu J, Farrell R, Mannazzu I, Budroni M, Maserti BE, Wisniewski ME, Migheli Q (2012) Identification of differentially expressed genes associated with changes in the morphology of *Pichia* on apple and peach fruit. FEMS Yeast Res 12:785–795

Fu H, Subramanian RR, Masters SC (2000) 14-3-3 proteins: structure, function, and regulation. Annu Rev Pharmacol Toxicol 40:617–647

Gancedo JM (2001) Control of pseudohyphae formation in *Saccharomyces cerevisiae*. FEMS Microbiol Rev 25:107–123

Giobbe S, Scherm B, Zara G, Budroni M, Migheli Q (2007) The strange case of a biofilm-forming strain of *Pichia fermentans*, which controls Monilinia brown rot on apple but is pathogenic on peach fruit. FEMS Yeast Res 7:1389–1398

Han-Yaku H, Naka W, Tajima S, Harada T, Nishikawa T (1996) Differential expression of the 45 kDa protein (actin) during the dimorphic transition of *Sporothrix schenckii*. J Med Vet Mycol 34:175–180

Hazelwood LA, Daran JM, van Maris AJ, Pronk JT, Dickinson JR (2008) The Ehrlich pathway for fusel alcohol production: a century of research on *Saccharomyces cerevisiae* metabolism. Rev Appl Environ Microbiol 74:2259–2266

Herbert B, Galvani M, Hamdan M, Olivieri E, MacCarthy J, Pedersen S, Righetti PG (2001) Reduction and alkylation of proteins in preparation of two-dimensional map analysis: why, when, and how? Electrophoresis 22:2046–2057

Hurtado CAR, Rachubinski RA (2002) YIBMH1 encodes a 14-3-3 protein that promotes filamentous growth in the dimorphic yeast *Yarrowia lipolytica*. Microbiol 148:3725–3735

Joshi CV, Ghormade V, Kunde P, Kulkarni P, Mamgain H, Bhat S, Paknikar KM, Deshpande MV (2010) Flocculation of dimorphic yeast *Benjaminiella poitrasii* is altered by modulation of NAD-glutamate dehydrogenase. Bioresour Technol 101:1393–1395

Jungblut PR, Holzhütter HG, Apweiler R, Schlüter H (2008) The speciation of the proteome. Chem Cen J 2:16–26

König S, Spinka M, Kutter S (2009) Allosteric activation of pyruvate decarboxylases. A never-ending story? J Mol Catal B Enzym 61:100–110

Lee BN, Elion EA (1999) The MAPKKK Ste11 regulates vegetative growth through a kinase cascade of shared signaling components. Proc Natl Acad Sci USA 96:12679–12684

Lima G, Arru S, De Curtis F, Arras G (1999) Influence of antagonist, host fruit and pathogen on the biological control of postharvest fungal diseases by yeasts. J Ind Microbiol Biotechnol 23:223–229

Liu X, Nie X, Ding Y, Chen J (2010) Asc1, a WD-repeat protein, is required for hyphal development and virulence in *Candida albicans*. Acta Biochim Biophys Sin (Shanghai) 42:793–800

Lorenz MC, Cutler NS, Heitman J (2000) Characterization of alcohol-induced filamentous growth in *Saccharomyces cerevisiae*. Mol Biol Cell 11:183–199

Maidan MM, Thevelein JM, Van Dijck P (2005) Carbon source induced yeast-to-hypha transition in *Candida albicans* is dependent on the presence of amino acids and on the G-protein-coupled receptor Gpr1. Biochem Soc Trans 33:291–293

Monteoliva L, Martinez-Lopez R, Pitarch A, Hernandez ML, Serna A, Nombela C, Albar AP, Gil C (2011) Quantitative proteome and acidic subproteome profiling of *Candida albicans* Yeast-to Hypha Transition. J Proteome Res 10:502–517

Moraes Nicola A, Vieira Andrade R, Silva-Pereira I (2005) Molecular chaperones in the *Paracoccidioides brasiliensis* transcriptome. Genet Mol Res 4:346–357

Olivera-Couto A, Aguila PS (2012) Eisosomes and plasma membrane organization. Mol Genet Genomics 287:607–620

Pan X, Harashima T, Heitman J (2000) Signal transduction cascades regulating pseudohyphal differentiation of *Saccharomyces cerevisiae*. Curr Opin Microbiol 3:567–572

Sanna ML, Zara S, Zara G, Migheli Q, Budroni M, Mannazzu I (2012) *Pichia fermentans* dimorphic changes depend on the nitrogen source. Fungal Biol 116:769–777

Schlüter H, Apweiler R, Holzhütter HG, Jungblut PR (2009) finding one's way in proteomics: a protein species nomenclature. Chem Cen J 3:11–21

Sharov AA, Dudekula DB, Ko MS (2005) A web-based tool for principal component and significance analysis of microarray data. Bioinformatics 21:2548–2549

Tylicki A, Siemieniuk M (2011) Thiamine and its derivatives in the regulation of cell metabolism. Postep Hig Med Dosw 65:447–469

Van Hemert MJ, Steensma YH, van Heusden GPH (2001) 14-3-3-proteins: key regulators of cell division, signaling and apoptosis. Bioassay 23:936–946

Vizcaino JA, Cote RG, Csordas A, Dianes JA, Fabregat A, Foster JM, Griss J, Alpi E, Birim M, Contell J, O'Kelly G, Schoenegger A, Ovelleiro D, Perez-Riverol Y, Reisinger F, Rios D, Wang R, Hermjakob H (2013) The Proteomics Identifications (PRIDE) database and associated tools: status in 2013. Nucleic Acids Res 41(D1):D1063–D1069

Vizcaíno JA, Deutsch EW, Wang R, Csordas A, Reisinger F, Ríos D, Dianes JA, Sun Z, Farrah T, Bandeira N, Binz PA, Xenarios I, Eisenacher M, Mayer G, Gatto L, Campos A, Chalkley RJ, Kraus HJ, Albar JP, Martinez-Bartolomé S, Apweiler R, Omenn GS, Martens L, Jones AR, Hermjakob H (2014) ProteomeXchange provides globally co-ordinated proteomics data submission and dissemination. Nature Biotechnol 30(3):223–226

Wisniewski ME, Wilson CL (1992) Biological control of postharvest diseases of fruits and vegetables. Recent Adv Hortsci 27:94–98

Zaragoza O, Gancedo JM (2000) Pseudohyphal growth is induced in *Saccharomyces cerevisiae* by a combination of stress and cAMP signalling. Antonie Van Leeuwenhoek 78:187–194

Zurita-Martinez SA, Cardenas ME (2005) Tor and cyclic AMP-protein kinase A: two parallel pathways regulating expression of genes required for cell growth. Eukaryot Cell 4:63–71